

A Vehicle Exhaust NO_x Electrochemical Sensor Based on Au-Yttria Stabilized Zirconia Nanocomposite

Junhua Wu^{1,*}, Fei Ge¹, and Yingjie Li²

¹ School of Automotive and Traffic Engineering, Nanjing Forestry University, Nanjing 210037, China

² College of Chemistry and Chemical Engineering, Shanghai University of Engineering Science, Shanghai 201620, China

*E-mail: 1103409684@qq.com

Received: 27 September 2016 / Accepted: 15 January 2017 / Published: 12 February 2017

Mixed potential sensor which is built on Yttria Stabilized Zirconia (YSZ) with a plain planar structure Au/YSZ/Pt has actual benefit among different kinds of NO_x sensors. To further sensing abilities, Au composites electrodes were taken a research on. The fact that adding YSZ into the Au electrode reduced in air the polarization resistance has been demonstrated by electrochemical impedance spectroscopy. The proposed porous Au-YSZ composite electrodes in a YSZ-based sensor have more positive effect than pure gold electrode based on the excellent performance. The proposed YSZ-based sensor could linearly detect NO₂ in the concentration between 50 to 400 ppm with a low detection limit of 20 ppm.

Keywords: NO_x electrochemical sensor; Gold, Yttria stabilized zirconia; Nanocomposite

1. INTRODUCTION

Various harmful gases, for example, hydrocarbons (HCs), nitrogen oxides (NO_x), carbon monoxide (CO), and hydrogen (H₂) are emitted by the combustion of fossil fuels or the leakage from gas tanks in automobiles and power plants by accident. NO_x is especially harmful that it causes adverse effect to respiratory system of human body and air pollution in urban area. Hence, to obtain appropriate control of combustion catalysts [1], there are urgent demands for high performance gas sensors monitoring NO_x sensitively and selectively [2].

In the last decade there have been plenty of studies and reports on different kinds of solid-electrolyte-based electrochemical NO_x-sensing devices since conditions were very harsh for operating

a practical sensor (multi-component gas mixtures, high humidity, high temperature). Among which the construction, overall survey and design of stabilized-zirconia-based NO_x sensors associated with metallic- or metal oxide-based sensing electrodes (SEs) is attracted lots attentions. Zirconia-based sensors is supposed to be highly sensitive and selective against NO₂ at operating temperatures above 800 °C since temperature of engine may be even 800–900 °C by chance when accelerating vehicle. It was found that a mixed-potential-type yttria-stabilized-zirconia (YSZ)-based sensor with a NiO-SE responded sensitively to NO₂ at temperatures of 800–850 °C [3, 4] when detecting a metal oxide-SE recently. The NiO-SE is supposed to be spruced at comparatively high temperatures of 1300–1400 °C [5] to be more sensitive and selective against NO₂ like this. To achieve reduction of the NiO-SE's temperature when sintered, several later attempts came into being by addition of a second component (dopant) to obtain the high performing capacity towards NO₂ [6-10]. Also, samaria-doped ceria (SDC) [11] or the β-alumina (2Na₂O–11Al₂O₃) [12] were taken into use as reference electrode.

To screen for NO_x, for instance, the couples Pt–(Au-oxide) [13], Pt–MnCr₂O₃ [14], or Pt–Au [15], the two electrodes have to display varying electro catalytic activity. Because of the formation of a mixed potential on the sensing electrode [14], the signal of a two electrode potentiometric sensor demonstrates non-Nernstian behaviors in a complex gas environment. This is latter associated to the duplication of reactions of parallel electrode coming up in the triple phase boundaries (TPB) [14, 16], for example, the electrochemical reduction (oxidation) of NO₂ (NO) and oxygen electrode reaction. NO₂ is entitled with higher sensitivity than that of NO. Besides, NO₂ and NO shows opposite responses by adopting the Au/Pt couple of electrodes associated with YSZ, negative for NO₂ [15, 17-20] and positive for NO.

A catalytic filter set on top of the electrodes [21] can help to avoid cross sensitivity to expel gases like hydrocarbons and CO. The catalytic layer is able to completely bring the molecules into CO₂ by oxidation without detected by the sensor. To achieve the thermodynamic equilibrium, the catalytic layer can also catalyze the NO oxidation into NO₂. Hence, the NO/NO₂ ratio only relies on the temperature of fixed partial pressure of oxygen. Furnished with a catalytic filter, we are to create a potentiometric sensor detecting NO₂ sensitively. Then, concentrations of overall NO_x, NO₂ and NO at oxygen partial temperature and constant temperature could be brought by the system.

This paper shows the implementation of NO₂ detection of YSZ-based solid state planar sensors with Au-composites the sensing electrodes and Pt a reference electrode. Its aim is to improve the quantity of TPBs of the sensing electrodes and the porosity, which are made up of Au mixed with ZrO₂ later. Electrochemical capabilities for the reaction of oxygen electrode were detected by impedance spectroscopy and made a comparison with those of pure Au sensing electrode. At last, sensing abilities for NO₂ at a temperature of 800 °C are also assessed.

2. EXPERIMENTS

2.1. Materials and apparatus

For creation of the sensor, a tape-casted YSZ (8 mol.%-doped Y₂O₃) plate (10 mm × 10 mm, 0.2 mm in thickness) was employed. Screen-printing (200 mesh) from a home-made ink which

contains solvent (ESL 404) 1 g mixed in a three-roll mill (Exakt 80E) for 10 mins, YSZ powder 4 g and organic binder 1.7 g (ESL V400A) established the functional and porous layer 5 mm × 5 mm of solid electrolyte (YSZ: $(\text{ZrO}_2)_{0.92}(\text{Y}_2\text{O}_3)_{0.08}$ brought by superconductive). After that, the samples were exsiccated at 120 °C in air for 15 min and spruced at 1100 °C for 2 h with a ramp of 5 °C/min. Adopting a commercial paste of Au (ESL 8880-H) as well as Pt (ESL 5545), gold and platinum electrodes of 4 mm length and 1 mm width were screen-printed on the surface of the YSZ layer. The electrodes was 2 mm near each other. The stored electrodes were desiccated at 120 °C further for 15 min and then sintered with a ramp of 5 °C/min for 2 h in air at 800 °C. The gold electrodes was labelled the sensing (Au-SE) electrode and the platinum electrodes was known as the reference (RE) electrode.

2.2. Sensor fabrication

The Au commercial paste and α -terpineol organic binder were mixed together, the result of which constituted an Au-SE, about 4 μm thick on average by screen-printed onto the front side of the YSZ. Then the Au-printed YSZ plates were spruced in air at 500 °C, 800 °C and 1100 °C for 2 h.

After calcination in air at 850 °C, specific area of YSZ powder, which was featured by adopting BET measurements with nitrogen (ASAP 2020) and laser granulometry (MASTERSIZER 2000 MALVERN), was 15 m^2/g but some area of ZrO_2 was 3.8 m^2/g . Mean particle size of agglomerates for ZrO_2 and YSZ respectively was 0.288 μm and 1.6 μm .

In a quartz tube, the fabricated planar sensors, linked to a conventional gas-flow apparatus, were established, set in an electric furnace. Features of the sensors for sensing gas were to be tested at 500 °C. The Pt-RE as well as the Au-SE was uncovered to the sample gas or to wet base gas at the same time (5 vol.% O_2 + 5 vol.% H_2O + N_2 balance). And each of parent gas (CO , CH_4 , C_3H_8 , NO and NO_2) with the base gas was diluted to make the sample gas. All of the concentrations of each gas tested were kept constant at 400 ppm in the sample gas for the selectivity tests. 100 ml/min was the gas-flow rate. In the NO_2 concentration range of 50–400 ppm, the dependence of the NO_2 sensitivity was assessed. With a digital electrometer (R8240, Advantest Corp., Japan), output of the electromotive force (*emf*) was taken as a sensing signal, which lies between the Pt-RE and the Au-SE of the sensor. The *emf* value of the sensor in the base gas (*emf*_{base}) and *emf* value in the sample gas (*emf*_{sample}) differ in that how sensitive ($\Delta\textit{emf}$) they are to each gas. By adoption of an electrochemical analyzer (PGSTAT30, AutoLab[®], The Netherlands), measurements of curves of current–voltage (polarization) can be displayed. Through adoption of a two-electrode configuration, the polarization curves were gauged at a constant scan rate of 2 mV/min between –20 as well as +100 mV in potentiodynamic mode.

3. RESULTS AND DISCUSSION

Figure. 1A display that the YSZ layer is extremely porous, probably due to the presence of evaporated binder and solvent in the initial paste. However, the surface of this layer evidences

percolation between micrometric YSZ grains ensuring bulk ionic conductivity. Figure 1B shows the XRD pattern of the prepared YSZ.

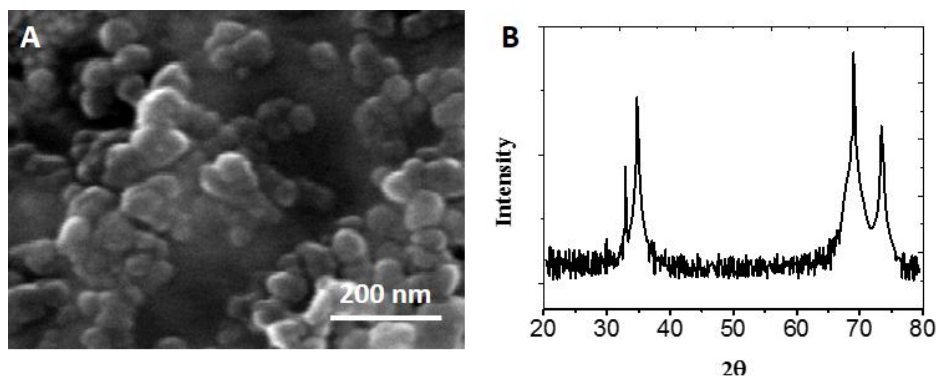


Figure 1. (A) Surface SEM image and (B) XRD pattern of the screen-printing YSZ layer.

Assessment of gas-sensing ability at different temperatures is paid great attention to by the current study. Figure 1 demonstrates the cross sensitivities of various gases for the sensors under the wet condition at 500 °C adopting Au-SEs assembled from the nano-structured precursor before sprued at respectively 1100 °C, 500 °C and 800 °C. Every tested YSZ-based sensor linked to the Au-SEs showed comparatively high NO₂ sensitivity; but to a large extent the results for selectivity against NO₂ differ. The sensor adopting the less-porous 500 °C-sprued Au-SE brought the best NO₂ sensitivity, but the reaction to NO₂ left few choices for a usable application. A relatively good reaction to CH₄ accompanied good sensitivity to NO₂. In spite of slightly lowering NO₂ sensitivity investigated, the NO₂ selectivity of the sensor referred to was obtained by the increase of the NiO-SE’s sintering temperature to 800 °C. The sensor connected to the dense and partially melted NiO-SE1100 °C-sintered showed good sensitivity to each tested gases.

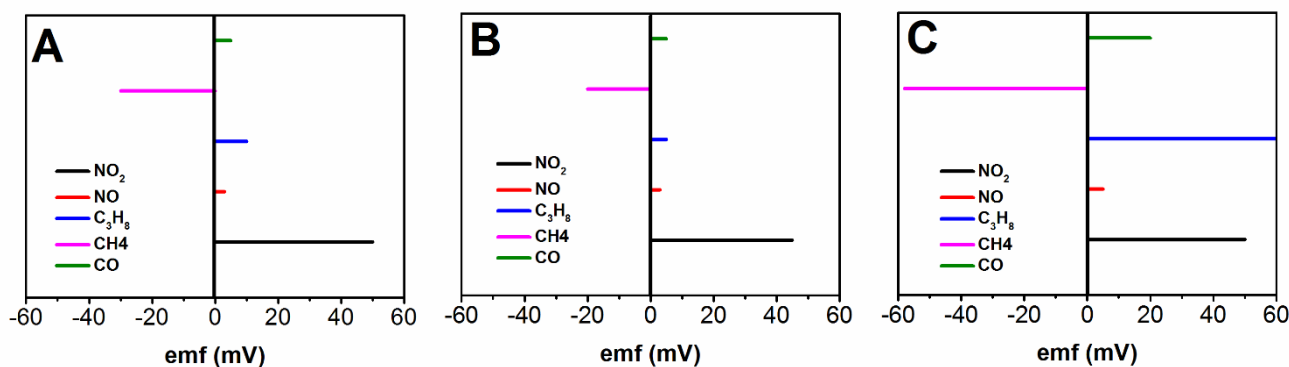


Figure 2. Cross sensitivities to different gases(400 ppm each) for the YSZ-based sensor under wet condition(5 vol.% water vapor) at 500 °C adopting all (A) 500 °C-, (B) 800 °C- and (C) 1000 °C-sintered Au-SEs.

Figure 3 displays a distinctive Nyquist plot of the AuY/AuY, AuZ/AuZ and Au/Au in air by 500 °C. For Au/Au sample, two specific semicircles that can be divided and decomposed are exhibited

by impedance spectra. Because of the obstruction of the conduction by the pores [22], in the high frequency (HF) domain, the first semicircle stands for the resistivity of the YSZ solid electrolyte layer (R_{SE}). In the low frequency (LF) scope (from 10^2 to 10^{-3} Hz), at the two symmetrical electrodes, the second contribution confirms with the whole polarization resistance (R_{POL}) connected with the kinetic electrode reactions [23, 24]. The electron transfer resistance (R_{ct}) was measured to be 422 Ω , 457 Ω and 466 Ω at the bare Au/Au, AuZ/AuZ and AuY/AuY, respectively, after the optimization of the equivalent and calculation. A significant increase of R_{ct} was observed when depositing AuY surface.

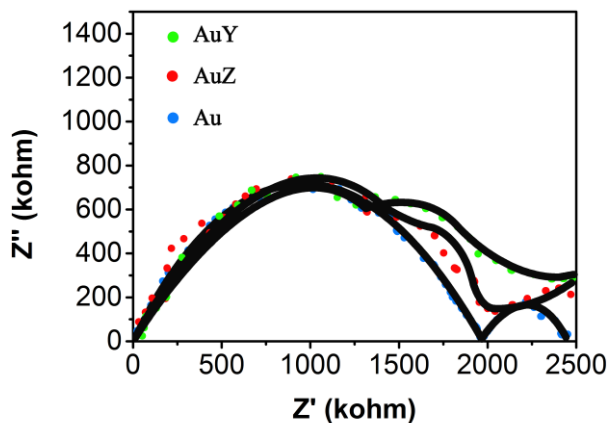


Figure 3. Certain Nyquist plot under experiment of Au–Au sample in air at 500 °C (numbers with arrow indicating \log_{10} of the frequency for measuring).

The resistance and the capacitance of the YSZ layer (Figure 4A), the parallel $R_{SE}C_{SE}$ element with R_{CE} and C_{SE} [25] can properly fits for the SE semi-circle. The YSZ layer's resistance is very good, around $2 \times 10^6 \Omega$ at 500 °C and is similar for three sensors (Figure 3B), which emphasizes the preparation method's high repeatability. Reports in the past studies [22] showed lower value than this one, which could be associated with the screen printed YSZ layer's high porosity. Around 1.2 eV is the activation energy, which is alike to the three symmetrical sensors, which accords with the value in the reports of porous YSZ membranes infused with 1 wt% Pt. The Arrhenius plot of the polarization resistance in air from 500 to 800 °C is demonstrated by Figure 4B. Generally, resistance of the YSZ layer is a order of magnitude higher than polarization resistance of the two symmetrical electrodes. AuZ/AuZ and Au/Au, the two samples, resemble with each other in values of polarization resistances and in the apparent activation energy. Hence, adding an insulating material to enhance the electrode porosity, for example, zirconia appears to change the oxygen electrode kinetic significantly. It is found that the presence of the oxide phase suppresses the cathodic electrode reaction.

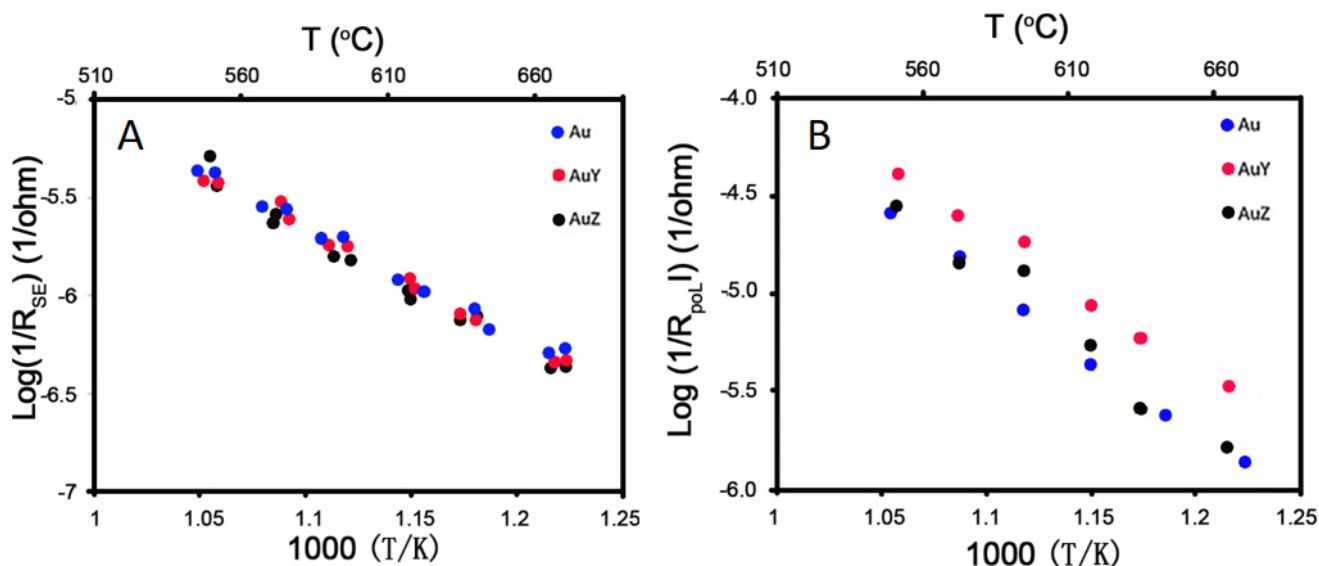


Figure 4. (A) Arrhenius plots of the solid electrolyte resistance (R_{SE}) (B) and the polarization resistance (R_{POL}) of the three symmetric sensors AuY/AuY, AuZ/AuZ and Au/Au.

In the base gas, OCV was monitored as a function of time (Figure 5) at 500 °C for evolution. These responses go in accordance with potential differences between the Au-SE and the Pt electrode. Because of the temperature regulation, initial signal varies abruptly. OCV values of the Au sensor increase greatly in the first 2 h, after that it will rise step by step. However, it cannot get to a steady-state forever. The Pt/Au sensor's OCV value is found to be +61 mV after 20 h on stream. The OCV between Pt electrodes and Au in oxygen atmosphere often results from the disagreement in the O₂ electrode kinetic rate connected with various oxygen activity. Behaviors of the two Au composites are alike, starting from an increase of the OCV and decaying gradually. The AuZ and AuY sensors' responses get to a steady +9 mV together with +3 mV respectively after on stream 5 and 12 h.

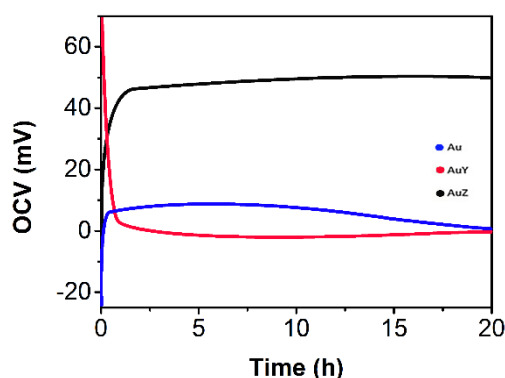


Figure 5. Sensor Pt/YSZ/SE baseline in 1.5% H₂O, 12% O₂ at 450 °C.

Figure 6 shows different reactions as well as recovery times of the three sensors after putting in 100 ppm NO₂ at 500 °C. AuY's response time is approximately 20 s, the shortest one, but the Au sensor spends about 40 s to respond and the sensor of AuZ needs 15 mins to react, the slowest one with

instable signal. To reassume the reaction at the beginning after the NO_2 exposure ends under $500\text{ }^\circ\text{C}$, several minutes are necessary, whatever the electrode is Au–Y composite could strongly cut thin recovery time for AuZ and Au which is 7 min instead of 40 min. A good adsorption of NO_2 onto the electrodes is likely to cause these long recovery time. The recovery time is reasonable on AuY and Au at a temperature of $550\text{ }^\circ\text{C}$ with a lower concentration of NO_2 (20 ppm). The linear response concentration of proposed AuY is between 50 to 400 ppm.

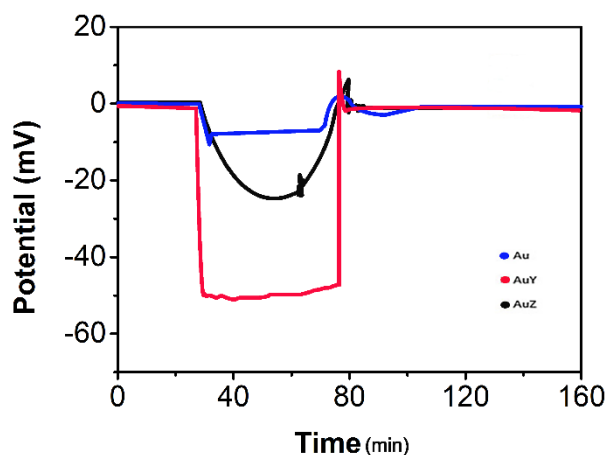


Figure 6. Responses (ΔV) of AuY, Au and AuZ sensors with 12% O_2 and 1.5% H_2O at $500\text{ }^\circ\text{C}$ to 100 ppm of NO_2 .

4. CONCLUSIONS

The study was aimed to take a research on the gold composite electrodes' impact on the capacities of a mixed potential Au/YSZ/Pt sensor. The competence of sensor referred to on response toward NO_2 was monitored at $500\text{ }^\circ\text{C}$. The fact that the polarization resistance is greatly decreased under the circumstances of Au–YSZ electrode is showed by electrochemical impedance measurements, which demonstrates that due to delocalization of YSZ's ionic conductivity to electrode response in the whole electrode volume, the electrochemical features of the oxygen electrode response can be optimized for the composite electrode of Au–YSZ only. Thus, it can be concluded that compared to pure gold electrode, in a YSZ-based sensor porous Au–YSZ composite electrodes display a beneficial effect.

References

1. S. Capone, A. Forleo, L. Francioso, R. Rella, P. Siciliano, J. Spadavecchia, D. Presicce and A. Taurino, *Journal of Optoelectronics and Advanced Materials*, 5 (2003) 1335
2. Y. Li, X. Li, Z. Tang, J. Wang, J. Yu and Z. Tang, *Sensors & Actuators B Chemical*, 223 (2015) 365
3. P. Elumalai and N. Miura, *Solid State Ionics*, 176 (2005) 2517
4. P.A. Rasheed, T. Radhakrishnan, P.K. Shihabudeen and N. Sandhyarani, *Biosensors &*

- bioelectronics*, 83 (2016) 361
5. P. Elumalai, J. Wang, S. Zhuiykov, D. Terada, M. Hasei and N. Miura, *Journal of The Electrochemical Society*, 152 (2005) H95
 6. V.V. Plashnitsa, T. Ueda and N. Miura, *International journal of applied ceramic technology*, 3 (2006) 127
 7. P. Elumalai, V.V. Plashnitsa, Y. Fujio and N. Miura, *Journal of The Electrochemical Society*, 156 (2009) J288
 8. S. Sundaravel, B. Venkatachalapathy, L. Sujatha, N.M. Sudharsan, T.S. Rao and T.M. Sridhar, “Yttria stabilized Zirconia sensors for biomedical detection of hydrogen sulphide”, Indo – Australian Conference on Biomaterials, Tissue Engineering, Drug Delivery System & Regenerative Medicine, 2015.
 9. L.Y. Woo, R.S. Glass, E.L. Brosha, R. Mukundan, F.H. Garzon, W.J. Buttner, M.B. Post, C. Rivkin and R. Burgess, *Ecs Transactions*, 45 (2013) 19
 10. M.J. Lee, J.H. Jung, K. Zhao, B.H. Kim, Q. Xu, B.G. Ahn, S.H. Kim and S.Y. Kim, *Journal of the European Ceramic Society*, 34 (2014) 1771
 11. C. Pijolat, G. Tournier and J.-P. Viricelle, *Sensors and Actuators B: Chemical*, 141 (2009) 7
 12. N. Guillet, R. Lalauze, J.-P. Viricelle, C. Pijolat and L. Montanaro, *Materials Science and Engineering: C*, 21 (2002) 97
 13. J. Zosel, D. Tuchtenhagen, K. Ahlborn and U. Guth, *Sensors and Actuators B: Chemical*, 130 (2008) 326
 14. C. Yin, Y. Guan, Z. Zhu, X. Liang, B. Wang, Q. Diao, H. Zhang, J. Ma, F. Liu and Y. Sun, *Sensors and Actuators B: Chemical*, 183 (2013) 474
 15. J. Gao, J.-P. Viricelle, C. Pijolat, P. Breuil, P. Vernoux, A. Boreave and A. Giroir-Fendler, *Sensors and Actuators B: Chemical*, 154 (2011) 106
 16. N. Miura, S. Zhuiykov, T. Ono, M. Hasei and N. Yamazoe, *Sensors and Actuators B: Chemical*, 83 (2002) 222
 17. J. Zhu, C.R. Pérez, T.S. Oh, R. Küngas and J.M. Vohs, *Journal of Materials Research*, 30 (2014) 357
 18. M. Fee, S. Ntais, A. Weck and E.A. Baranova, *Journal of Solid State Electrochemistry*, 18 (2014) 2267
 19. C.H. Hua and C.C. Chou, *Jpn.j.appl.phys*, 55 (2016) 080302
 20. S. Yu, C. Han, R. Li, H. Dai, S. He and L. Guo, *International Journal of Hydrogen Energy*, 39 (2014) 562
 21. J.-C. Yang and P.K. Dutta, *Sensors and Actuators B: Chemical*, 123 (2007) 929
 22. M. Kleitz and M. Steil, *Journal of the european ceramic society*, 17 (1997) 819
 23. L. Bultel, P. Vernoux, F. Gaillard, C. Roux and E. Siebert, *Solid State Ionics*, 176 (2005) 793
 24. T. Wang, R.F. Novak and R.E. Soltis, *Sensors and Actuators B: Chemical*, 77 (2001) 132
 25. W.-F. Zhang, P. Schmidt-Zhang and U. Guth, *Solid State Ionics*, 169 (2004) 121